International Journal of Nanoelectronics and Materials
IJNeaM
ISSN 198-5761 | E-ISSN 2232-1535

Synthesis of Zinc Oxide Nanoparticles via Cellar Spider Extract for Enhanced Functional Properties in Antimicrobial Activities

Jasni Mohamed Ismail[a], M. N. A. Uda[a,b,c,*], M. A. R. Irfan[b], M. K. R. Hashim[b] , Z. A. Arsat[b], Uda Hashim[a], Hafiza Shukor[d] ,M. N. Afnan Uda[e], N. H. Ibrahim[d], Shahidah Arina Shamsuddin[b], N. A. Parmin[a], M. Isa[a], Mohamad Zaim Mohamad Zain[d], R. A. Ilyas[f] and Tijjani Adam[a]

[a]*Institute of Nano Electronic Engineering, Universiti Malaysia Perlis, 01000 Kangar, Perlis, Malaysia.*
[b]*Faculty of Mechanical Engineering & Technology, Universiti Malaysia Perlis, Kampus Tetap Pauh Putra, 02600 Arau, Perlis, Malaysia.*
[c]*Centre of Excellence for Biomass Utilization, Universiti Malaysia Perlis, Arau 02600, Perlis, Malaysia.*
[d]*Faculty of Chemical Engineering & Technology, Universiti Malaysia Perlis, 02600 Arau, Perlis, Malaysia.*
[e]*Faculty of Engineering, Universiti Malaysia Sabah, 88400 Kota Kinabalu, Sabah, Malaysia.*
[f]*Faculty of Chemical and Energy Engineering, Universiti Teknologi Malaysia, Skudai 81310, Johor, Malaysia.*
**Corresponding author. Tel.: +604 988 5035; fax: +604 988 5034; e-mail: nuraiman@unimap.edu.my*

ABSTRACT

This study explores the green synthesis of zinc oxide nanoparticles (ZnO NPs) using cellar spider extracts as a sustainable alternative to traditional methods involving hazardous chemicals and radiation. The spider extracts effectively reduced zinc acetate dihydrate, yielding white precipitates indicative of ZnO NPs. Characterization through SEM revealed diverse morphologies, including spherical, rod-like, hexagonal, and uneven particles forming platelet-like aggregates. Further analyses, such as HPM, 3D nanoprofiler, and EDS, provided insights into size, shape, morphology, surface chemistry, thermal stability, and optical characteristics, quantifying the intended properties of the synthesized ZnO NPs. Antibacterial assays against *E. coli* and *B. subtilis* demonstrated significant antibacterial activity, affirming the nanoparticles' potential for antimicrobial applications. This green synthesis approach, validated through comprehensive characterization and quantitative measurements, offers a promising and environmentally friendly route for producing functional ZnO NPs.

Keywords: *Cellar spider extract, Green synthesis, Morphological study, Nanoparticles*

1. INTRODUCTION

The successful application of nanotechnology in agriculture increases the quantity and quality of agricultural products[1–4]. Using nano-pesticides and nano-fertilizers in agricultural management is good due to their higher effectiveness compared to conventional fertilizers [5]. Various types of nanoparticles with desired shapes and sizes have been created using various methods, including physical, chemical and biological procedures [6–8]. Because the size, structure and physical, chemical and biological characteristics involved are highly dependent on the dynamic process involved [9–12]. In general, the synthesis of ZnO NPs can be divided into three categories, namely chemical methods, physical methods and biological methods [13]. Researchers are working to develop simple, effective and reliable green chemical procedures for the synthesis of nanomaterials [14].

The process of green synthesis that is very beneficial to the environment is called the production of green nanoparticles. Because of its broad biological and chemical properties and its reduced potential harm when compared to chemically produced nanoparticles [15]. Due to its low cost, environmental friendliness, and scalability, green synthesis is found to be more advantageous than physical and chemical procedures. Plant extracts and microbes can be used in this green synthesis process. This technique is cheap, non-toxic and environmentally friendly [16]. Green synthesis has several limitations, including labor-intensive processes and reproducibility, but it is important to create reliable, sustainable and environmentally friendly synthesis methods to avoid the production of unwanted or toxic byproducts. Nanoparticle synthesis using the green synthesis method can build sustainable practices and reduce the production of hazardous chemical waste [17].

Arthropods, such as insects and arachnids, have been used in green synthesis due to their ability to produce a wide range of biologically active compounds, such as enzymes, pigments, and antimicrobial compounds. First, Arthropods are abundant and can be easily cultivated in large numbers, making them a sustainable source of bioactive compounds. Arthropods are efficient and able to produce large quantities of bioactive compounds in a relatively short period of time, making them a more efficient source of these compounds than other methods. Next, arthropods belong to a diverse group of animals that can produce a wide range of bioactive compounds, including enzymes, pigments, and antimicrobial compounds. Arthropod-based green synthesis methods are relatively low-cost and can be easily scaled up for commercial production. Furthermore, arthropod-based green synthesis methods are considered environmentally friendly as they do not

rely on harsh chemicals or solvents and can be performed under mild conditions. Finally, arthropod-derived bioactive compounds are often biocompatible, meaning they are less likely to cause adverse reactions in living organisms [18]. Cellar spiders are included in the group of arthropods that have many advantages for running green synthesis.

Zinc oxide nanoparticles (ZnO NPs) have received significant attention in various fields due to their unique properties and potential applications. ZnO NPs exhibit remarkable optical, electrical and catalytic properties, making them valuable in fields such as electronics, optoelectronics, catalysis, sensing and biomedical applications [19]. These nanoparticles have a wide band gap and large surface area, which contribute to their desirable properties and diverse applications. One of the main advantages of ZnO NPs is their ability to be synthesized using a variety of methods, including conventional and green synthesis approaches. Green synthesis methods, in particular, have gained popularity due to their environmentally friendly nature and potential for large-scale production without the use of toxic chemicals [20]. Such methods use natural resources, plant extracts, or biological agents as reducing and stabilizing agents, promoting the synthesis of sustainable and environmentally friendly nanoparticles.

Zinc oxide nanoparticles have gained popularity as cleaners and antimicrobials that usually have no negative side effects. Applications for zinc oxide nanoparticles include antibacterial, cell line research and dye degradation properties. ZnO NPs have a band gap of 3.37 eV, which is relevant for several applications in human health [21]. Zinc oxide nanoparticles have various antibacterial, antifungal and antiviral properties. Bacterial cell walls are permeable to zinc oxide nanoparticles, which can alter the structure of cell membranes and even kill cells. Their efficiency is due to both their large surface area to volume ratio and their nano size (Yin *et al.,* 2020). ZnO nanostructures have long been used as antibacterial agents in the healthcare industry, cosmetics, food storage, textile coating, and some environmental applications, although there is a lack of information on their toxicity and biological activity[22].

This study presents a novel approach to the green synthesis of zinc oxide nanoparticles (ZnO NPs) by utilizing cellar spider extracts as a sustainable alternative to conventional methods involving hazardous chemicals and radiation. Through the reduction of zinc acetate dihydrate, the spider extracts demonstrated efficacy, yielding distinct white precipitates indicative of ZnO NPs. The morphological diversity of the synthesized nanoparticles, including spherical, rod-like, hexagonal, and uneven particles forming platelet-like aggregates, was revealed through SEM characterization. In-depth analyses, such as HPM, 3D nanoprofiler, and EDS, provided comprehensive insights into size, shape, morphology, surface chemistry, thermal stability, and optical characteristics, quantifying the intended properties of the synthesized ZnO NPs. Antibacterial assays against E. coli and B. subtilis underscored significant antibacterial activity, affirming the nanoparticles' potential for antimicrobial applications. This innovative green synthesis approach, validated through comprehensive characterization and quantitative measurements, offers a promising and environmentally friendly route for producing functional ZnO NPs.

2. MATERIAL AND METHODS

2.1 Collection and Preparation of Cellar Spider Extract

A total of one hundred cellar spiders were rounded up and put alive inside of bottles. In order to get the extract of the cellar spider, one hundred milligrammes of the cellar spider were combined with ten millilitres of 0.1M sodium hydroxide (NaOH) in a beaker. Following the distillation of the mixture at 90 °C for one hour, it was allowed to cool before being centrifuged at 5000 rpm for twenty minutes [23]. During the process of separating the filtrate from the supernatant, which contained the extract we were looking for, we collected the supernatant. The procedure was carried out three more times so that a total amount of cellar spider extract containing 500 millilitres could be obtained. After keeping the extract at room temperature and covering it with aluminium foil for the night, it was then placed in the dark and maintained there for further synthesis in a beaker.

2.2 Synthesis of Zinc Oxide Nanoparticle Using Cellar Spider

Dissolving 46 g of Zinc acetate powder in 100 ml of distilled water yielded a 2.5M solution. 15 ml of the cellar spider extract from its preparation was put to a beaker with 30 ml of Zinc acetate solution. Aluminium foil shielded the beaker from light. After 2 hours of stirring, the cellar spider extract and zinc metal ions from Zinc acetate reacted, changing the solution's colour from light yellow to white. The mixture was transferred to an Eppendorf tube and centrifuged at 5000 rpm for 15 minutes. The supernatant was discarded, leaving the ZnO NP pellet in the tube. The particle was carefully rinsed with distilled water and centrifuged again at 5000 rpm for 15 minutes, discarding the supernatant. This washing procedure was repeated with 10% ethanol to eliminate contaminants and collect pure ZnO NPs pellets. After final washing and centrifugation, the pellet was dried overnight in an oven at 60 °C to produce the final product [24]. Pulverised dry material was kept in an airtight container at room temperature for future investigation.

2.3 Characterization of Zinc Oxide Nanoparticle

2.3.1 Scanning Electron Microscope (SEM)

The scanning electron microscopy (SEM) analysis was performed using a JEOL JSM6010LV instrument located in Tokyo, Japan. For the analysis, a single grain of powder was placed on a designated grid, and a current of 10

amperes was applied to it. Utilizing picture processing software, the particles were quickly visualized with clarity. To prepare the specimen for SEM analysis, a single drop of ZnO NPs powder was suspended in 50 ml of distilled water. After allowing sufficient time for the solution to be absorbed, 30 ml of the suspension was poured onto a clean wafer. The wafer was then observed at a working distance of 8 mm and an accelerating voltage of 5000 volts [25].

2.3.2 Energy-Dispersive X-Ray Spectroscopy (EDS)

Prepare a sample by spreading zinc oxide nanoparticles onto a carbon-coated copper grid. Place the grid in the sample holder of the EDS instrument. Use the instrument to direct a beam of electrons at the sample, causing the sample to emit X-rays. The emitted X-rays are detected by the instrument and used to determine the elemental composition of the sample found in the zinc oxide nanoparticle powder used [26].

2.3.3 High Power Microscope (HPM)

Using a high-pressure microscope (YJ-2007), 5 mg of ZnO NPs powder was used and suspended in 50 µl of distilled water. After absorbing for a while, 30 µl of solution was dropped on a clean wafer and dried it. Next, the wafer use for observation at 8 mm working distance. it is used for size, shape, and crystallinity characterization of the biogenic ZnO NPs. Images were taken at an acceleration voltage of 200 kV [27].

2.3.4 3D Nanoprofiler

The 3D nanoprofiler picture shows the algal extract and zinc oxide nanoparticles (ZnO NPs) sensor surfaces. The colour variation shows the height difference from the bottom to the top. A little quantity of ZnO NPs powder was suspended in 50 µl of distilled water for observation. The suspension absorbed for a while. Then, 30 ml of ZnO NPs solution was gently deposited onto a clean wafer to form a thin coating. The sample was seen at 8 mm. The nanoprofiler measured the algal extract and ZnO NPs layer heights during the observation. The 3D nanoprofiler picture showed height disparities throughout the sensing surface, helping to grasp the sample's surface shape and characteristics [11].

2.3.5 Antimicrobial Activities of Zinc Oxide Nanoparticle

The antimicrobial activities of zinc oxide nanoparticles (ZnO NPs) were investigated using various experimental procedures. Nutrient agar was prepared by dispersing 13 g of agar powder in 500 ml of distilled water, followed by autoclaving for sterilization. McFarland turbidity standards were created by mixing 1% sulfuric acid and 1% barium chloride to obtain specific optical densities, serving as references for bacterial suspension densities. Serial dilutions of ZnO NPs were conducted by transferring the nanoparticle solution into labeled Eppendorf tubes, progressively diluting it with sterile distilled water. The resulting solutions of different concentrations which were 1 mg/100 µL, 0.5 mg/100 µL, 0.25 mg/100 µL, 0.125 mg/100 µL, 0.063 mg/100 µL, and 0.0313 mg/100 µL, then used to assess the antimicrobial efficacy of ZnO NPs. The disc-diffusion assay was performed by spreading bacterial cultures onto agar plates, placing a filter paper disc on top, and adding ZnO NP samples drop by drop. The plates were incubated, and the size of the inhibition zone was measured. Statistical analysis was employed to calculate the sample mean and standard deviation, providing quantitative evaluation of the antimicrobial activity. Overall, these procedures allowed for the investigation and assessment of the antimicrobial properties of ZnO NPs [28–32].

3. RESULTS AND DISCUSSION

3.1 Overview of Synthesis Zinc Oxide Nanoparticle

Utilizing procedures that rely on visual identification enables one to ascertain the primary indications of the ZnO NPs that have been created. The change in colour of the reaction mixture that included a solution of zinc acetate dehydrate and cellar spider extract allowed for the creation of zinc oxide nanoparticles, which were denoted by the acronym ZnO NPs. As illustrated in Fig. 1, the reduction process to obtain ZnO NPs was confirmed by the color transition from light yellow to white in the reaction mixture containing Cellar spider and zinc acetate dehydrate. A colorless solution of zinc acetate dehydrate is first treated with subterranean spider extract, which results in the production of a color similar to light yellow. Next, the color changes to white, which is a white powder after drying to form ZnO NPs. [33].

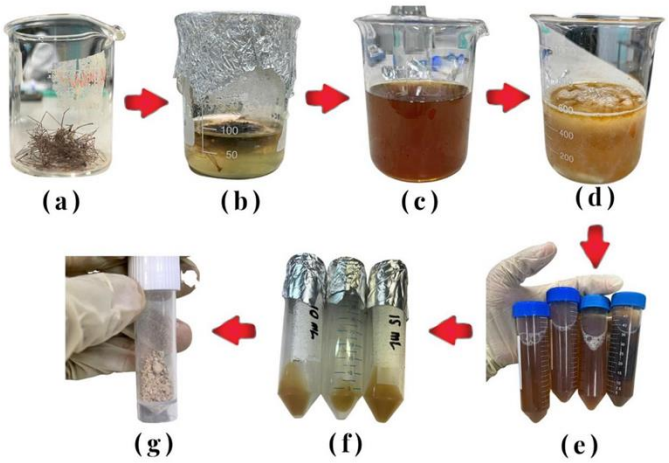

Figure 1. ZnO NPs synthesis via color changes in reaction mixtures: (a) 100mg Cellar Spider, (b) Cellar Spider + NaOH, (c) Cellar Spider extract, (d) pale yellow to white with zinc acetate dehydrate, (e) centrifugation preparation, (f) ZnO NPs pellet after 6000 rpm, (g) white ZnO NPs powder after 1-night drying.

3.2 Characterization of the Synthesized ZnO Nanoparticles

3.2.1 Scanning Electron Microscope (SEM)

Using a scanning electron microscope (SEM) with different magnifications, the size, shape, morphology, and surface chemistry of zinc oxide nanoparticles were further studied (Fig. 2). SEM micrographs revealed that the nanoparticles can have various shapes such as spherical, rod-like, hexagonal, or uneven, depending on their synthesis method and location. Surface patterns of the nanoparticles were observed, showing smooth or rough surfaces, as well as holes, cracks, or other imperfections (Fig. 2). Aggregation of particles was observed due to attractive forces, but closer examination revealed that the nanoparticles were spread out and exhibited platelet-like structures [34]. The topographic view indicated that the nanoparticles tended to cluster together and had a rough surface texture. ZnO nanoparticles derived from cellar spiders were found to be pure based on SEM images. The spherical shape of nanoparticles was particularly effective in antibacterial activity, as they could penetrate pathogens' cell walls rapidly. Therefore, ZnO nanoparticles synthesized from cellar spiders hold promise in clinical disease treatment [35]. Typically, ZnO nanoparticles range in size from 1 to 100 nanometers, with an average range of 5 to 50 nanometers. However, larger ZnO particles can also be generated, although they may be more appropriately called microparticles [36–38].

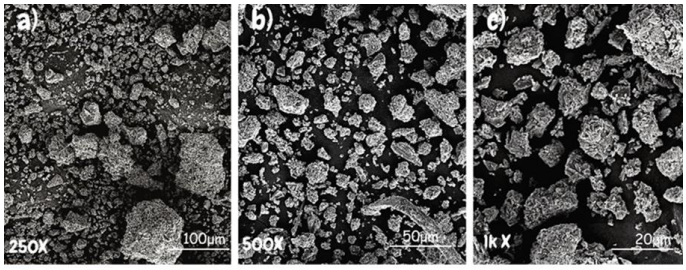

Figure 2. SEM image of biosynthesized zinc oxide nanoparticle. (a) raw powder of ZnO NPs at 250X (b) raw powder of ZnO NPs at 500X (c) raw powder of ZnO NPs at 1000X.

3.2.2 Energy-Dispersive X-ray Spectroscopy (EDS)

The EDS spectrum obtained from the analysis will display characteristic X-ray peaks corresponding to the elements present in the sample. In the case of ZnO nanoparticles, expect to see peaks corresponding to zinc (Zn) and oxygen (O). The presence and relative intensity of these peaks provide information about the elemental composition of the nanoparticles. The intensity of the peak in the EDS spectrum can provide a relative measure of elemental composition which can be seen from Fig. 3. The higher the intensity of a particular peak, the greater the concentration of the corresponding element in the sample. By comparing the intensity of zinc and oxygen peaks, it is possible to estimate the stoichiometry of ZnO nanoparticles. EDS analysis can also detect impurities or contaminants present in ZnO nanoparticles. If an additional peak is observed in the spectrum that does not correspond to Zn or O, it indicates the presence of other elements in the sample. This information is useful for evaluating the purity of nanoparticles [39].

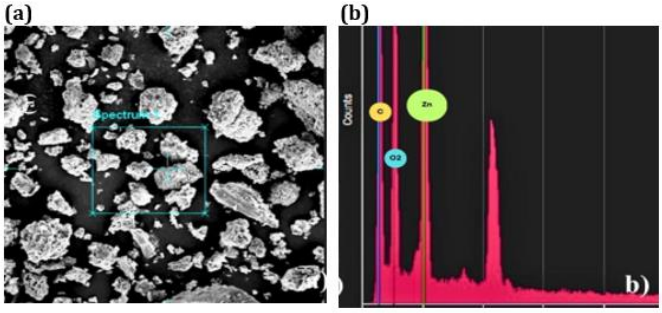

Figure 3. a) Image of ZnO NPs under SEM, b) The graph of molecule structure that content.

3.2.3 High Power Microscope (HPM)

A high-power microscope (HPM) was used to determine the structure of the Cellar spider extract and zinc oxide nanoparticles. The HPM provides high magnification and resolution for viewing small specimens. Fig. 4 displays photos of Cellar spider extracts taken with the microscope at different magnifications and illuminating conditions (bright field and dark field). The Cellar spider extract exhibits a conventional framework, while the zinc oxide nanoparticles appear as spherical particles resembling tiny balls or as hexagonal platelets with thin dimensions. These findings are consistent with previous research showing that zinc oxide nanoparticles are polydispersed and roughly spherical in shape [40].

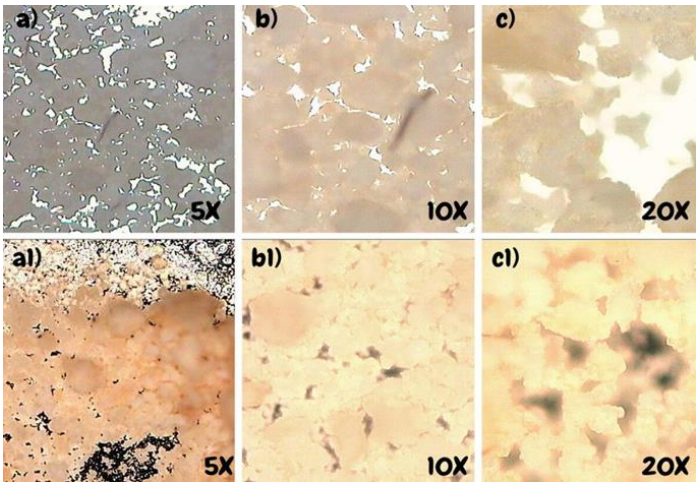

Figure 4. Image of Zinc Oxide Nanoparticle in (a 5x, b 10x and c 20x) under high power microscope in bright-field and (a1, b1 and c1) under dark field microscopy.

3.2.4 3D Nanoprofiler

Figure 5 presents a three-dimensional nano-profile of a ZnO NPs sensing surface, demonstrating the results of biosynthesized ZnO NPs. The maximum height observed was 129,987.5 nm, with an average height of 75,939.17 nm. The roughness analysis revealed two surfaces: one with a roughness of 121.0 nm and another with a

roughness of 32.6 nm. The surface area of the ZnO nanoparticles was measured to be 88.89 m2/g, with an average diameter of 7 nm. The surface roughness of the substrate influences the growth of ZnO nanostructures [41].

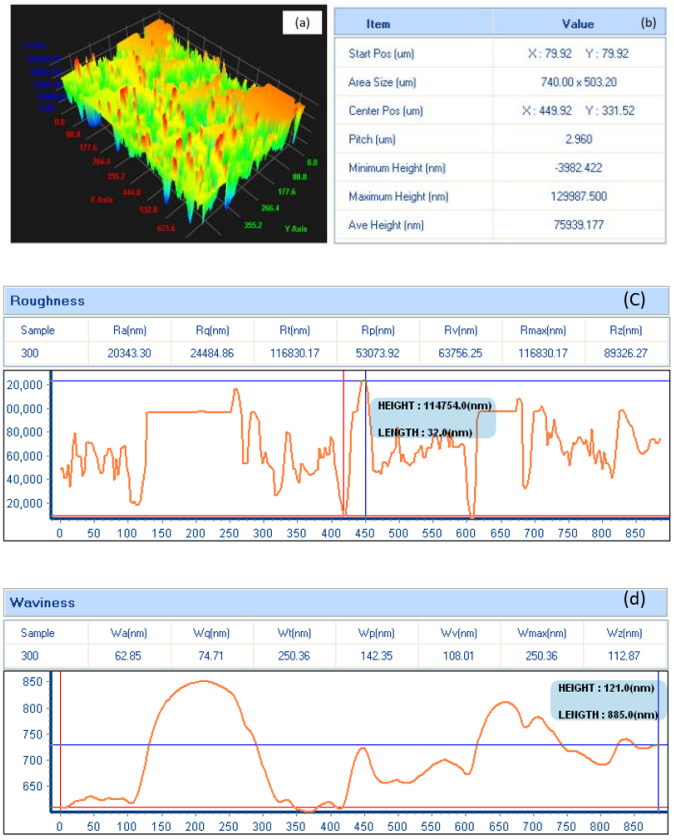

Figure 5. 3D nano-profile photography. 3D view (a) As you can see in the picture, the surface of ZnO NPs is made up of tiny circles or balls. Specification data (b); The table shows the height, area, and pitch of the ZnO NPs; (c) Roughness of the surface; (d) and waves.

3.2.5 Antimicrobial Activities of Zinc Oxide Nanoparticle

Figure 6 shown the zone of inhibition of the tested components is largest at a concentration of 1 mg/100 µL, indicating a direct proportional relationship between concentration and the zone of inhibition. As the concentration increases, the zone of inhibition also increases. The antimicrobial activity against E. coli produces a larger inhibition zone compared to B. subtilis due to the thinner cell wall in E. coli. E. coli's thin layer of peptidoglycan allows the tested components to permeate the cell wall, reducing cellular function and inhibiting growth. On the other hand, B. subtilis has a thick layer of peptidoglycan, limiting the penetration of the tested components and resulting in a smaller inhibition zone [42].

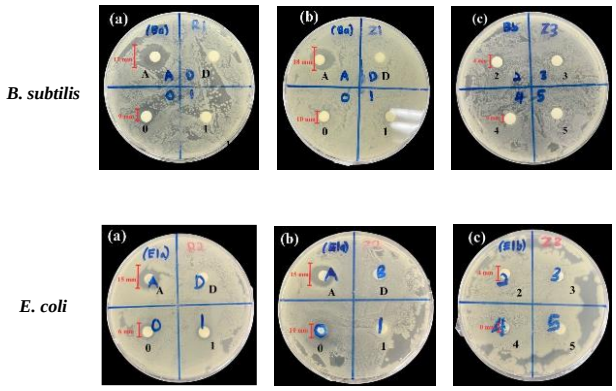

Figure 6. Antimicrobial activity of the tested components against B. subtilis and E. coli, for plate picture (a) (Amoxicilin (A), Distilled water (D), 1mg/100µL ZnO NPs (0) and 1mg/100µL Cellar spider extract (1)). For (b)(Amoxicilin (A), Distilled water (D), 1mg/100µL ZnO NPs (0) and 0.5 mg/100µL ZnO NPs (1)). For (c)(0.25 mg/100 µL ZnO NPs (2), 0.125 mg/100 µL ZnO NPs (3), 0.063 mg/100 µL ZnO NPs (4) and 0.0313 mg/100 µL ZnO NPs (5)).

Table 1 Measurement on zone of inhibition shown by ZnO NPs, Ampicillin, Raw cellar spider extract and Distilled water

Components	Concentration (mg/100µL)	Zone of Inhibition (mm)	
		B. subtilis	*E. coli*
ZnO NPs	1	9.0 (±1.5)	10 (±1.3)
	0.5	5 (±1.25)	6 (±1.25)
	0.25	4 (±1.0)	4 (±1.0)
	0.125	0	0
	0.063	0	0
	0.0313	0	0
Amoxicilin	50	16.0 (±2.0)	18.0 (±1.5)
Cellar Spider Extract	1	6.0 (±1.0)	7.0 (±1.0)
	0.5	0	0
Distilled Water	0	0	0

The P-value seen in each data parameter, which shows the statistical significance of the difference between antimicrobial components and each concentration, was found to be P = 8.32985×10^{-21} on ZnO NPs, P = 9.24336×10^{-6} on Amoxicillin, and P = 7.07225×10^{-9} on Raw Cellar Spider. The P-value indicates the level of statistical significance of the difference observed between treatments. In this case, the P-values were all less than 0.05, indicating that the observed difference in distance between treatments was statistically significant at the given significance level.

The values enclosed in parentheses in Table 1 indicate the acceptable range, denoting the plus-minus variation or uncertainty associated with the inhibition zone measurements. This range is useful for assessing the reliability and consistency of the results obtained. The zone of inhibition of all tested components shows the largest at 1 mg/100 µL, which is the highest concentration. This indicates a direct proportional relationship between concentration and the zone of inhibition. As the concentration increases, the zone of inhibition also increases. Furthermore, the antimicrobial

activity of the tested components against *E. coli* produces a larger inhibition zone compared to *B. subtilis,* where the inhibition zone is smaller. This difference can be attributed to the thickness of the cell wall in E. coli, which is thinner than in *B. subtilis. E. coli* consists of a thin layer of peptidoglycan between the inner and outer layers of the lipid membrane [42]. Therefore, the tested components have increased accessibility to permeate the cell wall of *E. coli,* leading to reduced cellular function and inhibited growth. In contrast, *B. subtilis* has a thick layer of peptidoglycan in its cell wall, which restricts the penetration of the tested components and results in a smaller inhibition zone.

CONCLUSION

In conclusion, our investigation unveils a sustainable approach for synthesizing zinc oxide nanoparticles (ZnO NPs) using cellar spider extracts, marked by observable color changes during the reaction. The synthesized ZnO NPs showcase diverse morphologies, spanning spherical, rod-like, hexagonal, and uneven particles. Rigorous characterizations employing SEM, EDS, HPM, and 3D Nanoprofiler yield quantitative data on size, shape, surface chemistry, and topography. Antimicrobial assays indicate concentration-dependent inhibition zones against both *E. coli* and *B. subtilis*, with the highest concentration (1 mg/100 µL) eliciting significant effects. Statistical analyses underscore the robustness of the results, with low P-values (8.33x10-21 for ZnO NPs, 9.24x10-6 for Amoxicillin, and 7.07x10-9 for Raw Cellar Spider). Moreover, the 3D Nanoprofiler provides a detailed nano-profile, revealing a maximum height of 129,987.5 nm, an average height of 75,939.17 nm, and surface roughness characteristics. Overall, our study presents a visually guided green synthesis method for ZnO NPs, offering diverse morphologies and substantiating antimicrobial efficacy through a comprehensive array of numerical analyses.

ACKNOWLEDGMENTS

We would like to express our sincere appreciation to the Institute of Nanoelectronics Engineering and the Faculty of Chemical Engineering Technology at the University of Malaysia Perlis, as well as to the technical workers involved. Their contributions and support have been vital in the successful completion of our project, and we are honored to have had the opportunity to collaborate with such esteemed institutions and individuals.

REFERENCES

[1] S. C. B. Gopinath, S. Ramanathan, K. Hann Suk, M. Ee Foo, P. Anbu, M. N. A. Uda, Engineered nanostructures to carry the biological ligands, MATEC Web Conf. 150 (2018) 06002. https://doi.org/10.1051/matecconf/201815006002.

[2] M. N. A. Uda, T. Adam, C. M. Hasfalina, S. Faridah, I. Zamri, U. Hashim, S. A. Ariffin, Reviewed Immunosensor Format Using Nanomaterial for Tungro Virus Detection, Adv. Mater. Res. 832 (2014) 410–414. https://doi.org/10.4028/www.scientific.net/AMR.832.410.

[3] M. N. A. Uda, C. M. Hasfalina, A. A. Samsuzanaa, S. Faridah, I. Zamri, B. S. Noraini, W. N. Sabrina, U. Hashim, S. C. B. Gopinath, Immunosensor development formatting for tungro disease detection using nano-gold antibody particles application, AIP Conf. Proc. 1808 (2017). https://doi.org/10.1063/1.4975290.

[4] M. N. A. Uda, C. M. Hasfalina, A. A. Samsuzana, U. Hashim, S. A. B. Ariffin, I. Zamri, W. Nur Sabrina, B. B. Siti Noraini, S. Faridah, M. Mazidah, S. C. B. Gopinath, Immunosensor development for rice tungro bacilliform virus (RTBV) detection using antibody nano-gold conjugate, AIP Conf. Proc. 1808 (2017) 1–9. https://doi.org/10.1063/1.4975291.

[5] N. A. Hasmin, Z. A. Zainol, R. Ismail, J. Matmin, Disclosure of nanomaterials under nanotechnology product inventory, voluntary certification, and voluntary labelling, Pertanika J. Soc. Sci. Humanit. 29 (2021) 157–174. https://doi.org/10.47836/PJSSH.29.1.09.

[6] M. N. A. Uda, U. Hashim, C. B. Subash Gopinath, M. N. Afnan Uda, N. A. Parmin, H. Adam, N. H. Ibrahim, Spectrophotometric Analysis Assay for the Measurement of Arsenic Using Nanocomposite of Silica and Graphene, IOP Conf. Ser. Mater. Sci. Eng. 743 (2020). https://doi.org/10.1088/1757-899X/743/1/012016.

[7] M. N. A. Uda, S. C. B. Gopinath, U. Hashim, N. H. Halim, N. A. Parmin, M. N. Afnan Uda, P. Anbu, Production and characterization of silica nanoparticles from fly ash: conversion of agro-waste into resource, Prep. Biochem. Biotechnol. 51 (2021) 86–95. https://doi.org/10.1080/10826068.2020.1793174.

[8] T. Balasubramaniam, A. H. A. Bakar, M. N. A. Uda, U. Hashim, N. A. Parmin, A. Anuar, M. A. A. Bakar, M. N. Afnan Uda, M. K. Sulaiman, Potential of Syntesized Silica Nanoparticles (Si-NPs) using Corn Cob for Arsenic Heavy Metal Removal, IOP Conf. Ser. Mater. Sci. Eng. 864 (2020). https://doi.org/10.1088/1757-899X/864/1/012187.

[9] M. N. A. Uda, S. C. B. Gopinath, U. Hashim, M. N. Afnan Uda, N. H. Ibrahim, N. A. Parmin, N. H. Halim, P. Anbu, Simple and Green Approach Strategy to Synthesis Graphene Using Rice Straw Ash, IOP Conf. Ser. Mater. Sci. Eng. 864 (2020). https://doi.org/10.1088/1757-899X/864/1/012181.

[10] A. H. M, M. N. A. Uda, S. C. B. Gopinath, Z. A. Arsat, F. Abdullah, M. F. A. Muttalib, M. K. R. Hashim, U. Hashim, M. N. A. Uda, A. R. W. Yaakub, N. H. Ibrahim, N. A. Parmin, T. Adam, Green route synthesis of antimicrobial nanoparticles using sewage alga bloom, Mater. Today Proc. (2023).

https://doi.org/10.1016/j.matpr.2023.01.008.
[11] H. M. Azwatul, M. N. A. Uda, S. C. B. Gopinath, Z. A. Arsat, F. Abdullah, M. F. A. Muttalib, M. K. R. Hashim, U. Hashim, M. Isa, M. N. A. Uda, A. Radi Wan Yaakub, N. H. Ibrahim, N. A. Parmin, T. Adam, Synthesis and characterization of silver nanoparticle using sewage algal bloom extract using visual parameter analysis, Mater. Today Proc. (2023). https://doi.org/10.1016/j.matpr.2023.01.004.
[12] H. M. Azwatul, M. N. A. Uda, S. C. B. Gopinath, Z. A. Arsat, F. Abdullah, M. F. A. Muttalib, M. K. R. Hashim, U. Hashim, M. Isa, M. N. A. Uda, A. Radi Wan Yaakub, N. H. Ibrahim, N. A. Parmin, T. Adam, Plant-based green synthesis of silver nanoparticle via chemical bonding analysis, Mater. Today Proc. (2023). https://doi.org/10.1016/j.matpr.2023.01.005.
[13] L. Wei, J. Lu, H. Xu, A. Patel, Z.S. Chen, G. Chen, Silver nanoparticles: Synthesis, properties, and therapeutic applications, Drug Discov. Today. 20 (2015) 595–601. https://doi.org/10.1016/j.drudis.2014.11.014.
[14] M. N. A. Uda, S. C. B. Gopinath, U. Hashim, M. N. Afnan Uda, N. A. Parmin, N. H. Halim, P. Anbu, Novelty Studies on Amorphous Silica Nanoparticle Production from Rice Straw Ash, IOP Conf. Ser. Mater. Sci. Eng. 864 (2020). https://doi.org/10.1088/1757-899X/864/1/012021.
[15] P. Anbu, S. C. B. Gopinath, H. Shik, C. Lee, Temperature-dependent green biosynthesis and characterization of silver nanoparticles using balloon fl ower plants and their antibacterial potential, J. Mol. Struct. 1177 (2019) 302–309. https://doi.org/10.1016/j.molstruc.2018.09.075.
[16] G. Mehdi, Green synthesis, characterization and antimicrobial activity of silver nanoparticles (AgNPs) using leaves and stems extract of some plants, Adv. J. Chem. A. 2 (2019) 266–275. https://doi.org/10.33945/sami/ajca.2019.4.1.
[17] S. Gobalakrishnan, N. Chidhambaram, M. Chavali, Role of greener syntheses at the nanoscale, Handb. Greener Synth. Nanomater. Compd. Vol. 1 Fundam. Princ. Methods. (2021) 107–134. https://doi.org/10.1016/B978-0-12-821938-6.00004-9.
[18] A. Lateef, S. A. Ojo, J. A. Elegbede, The emerging roles of arthropods and their metabolites in the green synthesis of metallic nanoparticles, Nanotechnol. Rev. 5 (2016) 601–622. https://doi.org/10.1515/ntrev-2016-0049.
[19] A. Sirelkhatim, S. Mahmud, A. Seeni, N. H. M. Kaus, L. C. Ann, S. K. M. Bakhori, H. Hasan, D. Mohamad, Review on zinc oxide nanoparticles: Antibacterial activity and toxicity mechanism, Nano-Micro Lett. 7 (2015) 219–242. https://doi.org/10.1007/s40820-015-0040-x.
[20] T. U. Doan Thi, T. T. Nguyen, Y. D. Thi, K. H. Ta Thi, B. T. Phan, K. N. Pham, Green synthesis of ZnO nanoparticles using orange fruit peel extract for antibacterial activities, RSC Adv. 10 (2020) 23899–23907. https://doi.org/10.1039/d0ra04926c.
[21] N. A. Al-Dhabi, M. V. Arasu, Environmentally-friendly green approach for the production of zinc oxide nanoparticles and their anti-fungal, ovicidal, and larvicidal properties, Nanomaterials. 8 (2018). https://doi.org/10.3390/nano8070500.
[22] A. C. Burduşel, O. Gherasim, A. M. Grumezescu, L. Mogoantă, A. Ficai, E. Andronescu, Biomedical applications of silver nanoparticles: An up-to-date overview, Nanomaterials. 8 (2018) 1–25. https://doi.org/10.3390/nano8090681.
[23] L. Azeez, A. Lateef, S. A. Adebisi, A. O. Oyedeji, Novel biosynthesized silver nanoparticles from cobweb as adsorbent for Rhodamine B: equilibrium isotherm, kinetic and thermodynamic studies, Appl. Water Sci. 8 (2018) 1–12. https://doi.org/10.1007/s13201-018-0676-z.
[24] M. Naseer, U. Aslam, B. Khalid, B. Chen, Green route to synthesize Zinc Oxide Nanoparticles using leaf extracts of Cassia fistula and Melia azadarach and their antibacterial potential, Sci. Rep. 10 (2020) 1–10. https://doi.org/10.1038/s41598-020-65949-3.
[25] M. N. A. Uda, S. C. B. Gopinath, U. Hashim, N. H. Halim, N. A. Parmin, M. N. Afnan Uda, A. Tijjani, A. Periasamy, Silica and graphene mediate arsenic detection in mature rice grain by a newly patterned current – volt aptasensor, Sci. Rep. 11 (2021) 1–13. https://doi.org/10.1038/s41598-021-94145-0.
[26] S. Nasrazadani, S. Hassani, Modern analytical techniques in failure analysis of aerospace, chemical, and oil and gas industries, Elsevier Ltd., 2015. https://doi.org/10.1016/B978-0-08-100117-2.00010-8.
[27] N. M. Shamhari, B. S. Wee, S. F. Chin, K. Y. Kok, Synthesis and characterization of zinc oxide nanoparticles with small particle size distribution, Acta Chim. Slov. 65 (2018) 578–585. https://doi.org/10.17344/acsi.2018.4213.
[28] P. Roy, B. Das, A. Mohanty, S. Mohapatra, Green synthesis of silver nanoparticles using azadirachta indica leaf extract and its antimicrobial study, Appl. Nanosci. 7 (2017) 843–850. https://doi.org/10.1007/s13204-017-0621-8.
[29] U. Kesici, M. Demirci, S. Kesici, Antimicrobial effects of local anaesthetics, Int. Wound J. 16 (2019) 1029–1033. https://doi.org/10.1111/iwj.13153.
[30] B. M. Khan, J. Bakht, M. Shafi, Screening of leaves extracts from Calamus aromaticus for their antimicrobial activity by disc diffusion assay, Pak. J. Pharm. Sci. 30 (2017) 793–800.
[31] M. Hamelian, M. M. Zangeneh, A. Amisama, K. Varmira, H. Veisi, Green synthesis of silver nanoparticles using Thymus kotschyanus extract and evaluation of their antioxidant, antibacterial and cytotoxic effects, Appl. Organomet. Chem. 32 (2018) 1–8. https://doi.org/10.1002/aoc.4458.
[32] M. N. A. Uda, S. C. B. Gopinath, N. H. Ibrahim, M. K. R. Hashim, M. A. Nuradibah, M. N. Salimi, T. E. Shen, O. Y. Fen, M. A. M. Akhir, U. Hashim, Preliminary Studies on Antimicrobial Activity of Extracts from Aloe Vera Leaf, Citrus Hystrix Leaf, Zingiber Officinale and Sabah Snake Grass Against Bacillus Subtilis, MATEC Web Conf. 150 (2018) 2–5.

https://doi.org/10.1051/matecconf/201815006042.

[33] Sachin, Jaishree, N. Singh, R. Singh, K. Shah, B.K. Pramanik, Green synthesis of zinc oxide nanoparticles using lychee peel and its application in anti-bacterial properties and CR dye removal from wastewater, Chemosphere. 327 (2023) 138497. https://doi.org/10.1016/j.chemosphere.2023.138497.

[34] W. Widiyastuti, S. Machmudah, T. Nurtono, S. Winardi, R. Balgis, T. Ogi, K. Okuyama, Morphology and optical properties of zinc oxide nanoparticles synthesised by solvothermal method, Chem. Eng. Trans. 56 (2017) 955–960. https://doi.org/10.3303/CET1756160.

[35] M. Ozdal, S. Gurkok, Recent advances in nanoparticles as antibacterial agent, ADMET DMPK. 10 (2022) 115–129. https://doi.org/10.5599/admet.1172.

[36] U. Hashim, M. F. M. Fathil, M. K. M. Arshad, S. C. B. Gopinath, M. N. A. Uda, Characterization of zinc oxide thin film for pH detector, AIP Conf. Proc. 1808 (2017). https://doi.org/10.1063/1.4975253.

[37] M. N. A. Uda, T. Adam, U. Hashim, A. B. Mosbah, M. N. A. Uda, MPTES decorated IDE for arsenic (AS) selective detection, AIP Conf. Proc. 2339 (2021). https://doi.org/10.1063/5.0044562.

[38] U. Hashim, T. Adam, N. A. K. H. Ehfaed, M. N. A. Uda, M. N. A. Uda, Quantitative lead (Pb+) ion detection via modified silicon nanowire, AIP Conf. Proc. 2339 (2021). https://doi.org/10.1063/5.0044568.

[39] S. Nagarajan, K. Arumugam Kuppusamy, Extracellular synthesis of zinc oxide nanoparticle using seaweeds of gulf of Mannar, India, J. Nanobiotechnology. 11 (2013) 1–11. https://doi.org/10.1186/1477-3155-11-39.

[40] D. Jain, Shivani, A. A. Bhojiya, H. Singh, H. K. Daima, M. Singh, S. R. Mohanty, B. J. Stephen, A. Singh, Microbial Fabrication of Zinc Oxide Nanoparticles and Evaluation of Their Antimicrobial and Photocatalytic Properties, Front. Chem. 8 (2020) 1–11. https://doi.org/10.3389/fchem.2020.00778.

[41] C. Zhou, Y. Wang, L. Du, H. Yao, J. Wang, G. Luo, Precipitation Preparation of High Surface Area and Porous Nanosized ZnO by Continuous Gas-Based Impinging Streams in Unconfined Space, Ind. Eng. Chem. Res. 55 (2016) 11943–11949. https://doi.org/10.1021/acs.iecr.6b03348.

[42] E. J. Hayhurst, L. Kailas, J. K. Hobbs, S. J. Foster, Cell wall peptidoglycan architecture in Bacillus subtilis, Proc. Natl. Acad. Sci. U. S. A. 105 (2008) 14603–14608. https://doi.org/10.1073/pnas.0804138105.